Journal of Advanced Ceramics
2019, **8**(1): 102–111
https://doi.org/10.1007/s40145-018-0298-9

ISSN 2226-4108
CN 10-1154/TQ

Research Article

ZrB_2 particles reinforced glass coating for oxidation protection of carbon/carbon composites

Cuiyan LI*, Guibiao LI, Haibo OUYANG, Jing LU

School of Materials Science & Engineering, Shaanxi University of Science & Technology, Xi'an 710021, China

Received: June 6, 2018; Revised: September 30, 2018; Accepted: October 1, 2018

Abstract: A dense ZrB_2 particles reinforced glass (ZrB_2/SiO_2) coating was prepared on the SiC coated carbon/carbon composites by a facile sol-dipping approach. The prepared ZrB_2/SiO_2 coating could protect the composites from being oxidized for 160 h at 1773 K with a weight loss of 6.9 mg/cm^2. The flexural strength retention ratio of the ZrB_2/SiO_2 coated composites is 87% after oxidation for 160 h at 1773 K. The continuous SiO_2 glass layer embedded with the submicron $ZrSiO_4$ particles was formed during oxidation. This was helpful to lower the diffusion rate of oxygen and improve the stability of SiO_2 glass film, thus improving the oxidation resistance of the coated samples. After thermal cycles between 1773 K and room temperature for 15 times, penetrated cracks formed in the coating. The weight loss of the ZrB_2/SiO_2 coated sample presented linear relationship, and the final weight loss per unit area was 6.35 mg/cm^2. The generation of the penetrative cracks and the debonded coating interface resulted in the failure of the ZrB_2/SiO_2 coating.

Keywords: ZrB_2/SiO_2 coating; silica sol; dipping; oxidation resistance

1 Introduction

Zirconium diboride (ZrB_2) is an attractive thermal protection material for carbon/carbon (C/C) composites due to its high melting temperatures, good thermal conductivities, and outstanding thermochemical properties [1,2]. Researches showed that introducing silicide into ZrB_2 can significantly promote the oxidation protection ability of ZrB_2 coating because of the formation of a stable compound silicate glass layer. In order to improve the oxidation protection for C/C and C/SiC composites, some efforts have been devoted to prepare ZrB_2–silicide coatings, such as ZrB_2–SiC [3,4], ZrB_2–$MoSi_2$ [5], SiC–$MoSi_2$–ZrB_2 [6], ZrB_2–$TaSi_2$ [7], SiC/ZrB_2–SiC/SiC [8], ZrB_2–$CrSi_2$–SiC–Si/SiC [9], and ZrB_2–SiC–Si/B [10] coatings, improving the oxidation protection for C/C and C/SiC composites.

Dispersion of ceramic particles can improve oxidation resistance of ZrB_2–silicide coating [11,12]. Uniform distribution of ceramic particles can make silicide more effective in providing the silica-rich glass, leading to the formation of the protective silica layer during oxidation as soon as possible. In order to further improve the distribution of ZrB_2 in the coatings, many techniques have been developed to prepare the ZrB_2–silicide coatings. Pourasad *et al.* [13] prepared a SiC–ZrB_2 coating on a graphite substrate by a novel pack cementation technique at 1873 K with Zr, Si, and B_4C powders. The SiC–ZrB_2 coating could efficiently enhance oxidation resistance of graphite. Li *et al.* [14] prepared a SiC–ZrB_2–ZrC coating on C/C composites

* Corresponding author.
E-mail: licuiyan@sust.edu.cn, cuiyan.lee@163.com

by pack cementation using ZrC, B_4C, and Si as the precursor powder. The ZrB_2 and ZrC were homogeneously dispersed in the coating. The multiphase coating showed the better oxidation resistance at a higher oxygen partial pressure. Wang *et al.* [15] prepared a gradient SiC–ZrB_2–$MoSi_2$ coating on SiC coated C/C composites using supersonic plasma spraying. Its excellent anti-oxidation behavior was due to the formation of zircon and SiO_2, which would flow to seal the extension of the cracks. Niu *et al.* [16] fabricated ZrB_2–$MoSi_2$ composite coatings by low-pressure plasma spray. $MoSi_2$ presented uniform distribution in the ZrB_2–$MoSi_2$ coating. The fine distribution of sufficient $MoSi_2$ in the matrix and dense microstructure of the ZrB_2–$MoSi_2$ coating contributed to its excellent high-temperature oxidation resistance. Yang *et al.* [17] prepared the ZrB_2/SiC coating on C/SiC composite surface by slurry painting and chemical vapor deposition. Results showed that the coating retained 37.4% of original flexural strength and provided longtime protection for C/SiC composites at 1973 K.

However, ZrB_2 particles were coarse in the coating due to the high-temperature sintering in pack cementation process. Many oxides and pores have been found in the coating which resulted from the oxidation of ZrB_2 and silicide particles in the plasma spray process. Our previous works have studied a self-healing ZrB_2–SiO_2 coating with dispersed submicron ZrB_2 particles prepared by infiltrating silica sol into a porous ZrB_2 layer. The dispersed ZrB_2 particles separate the silica gel into small pieces, which can reduce the shrinkage stress and act as pinning centers to restrain the formation of cracks [18].

Silica sol is considered as an efficient dispersant for ceramic powders. The silica sol can enhance the stability of silicon carbide and zirconia suspensions [19]. The dispersion and stabilization of ceramic powders in the silica sol are essential for the wet processing of high-performance ceramics. Furthermore, silica sol can not only provide high bond strength for ceramic bodies due to its conversion to a solid gel at relatively low temperature but also improve sinterability of ceramic powders and promote the densification of ceramics [20,21]. Therefore, silica sol has successfully been employed to fabricate the ceramic coatings [18,22]. Recently, dip-coating techniques were also developed to prepare ceramic coatings. Ma and Cai [23] prepared a tri-layer of mullite/$Y_2Si_2O_7$/(70wt%$Y_2Si_2O_7$+30wt%Y_2SiO_5) coating on the C/SiC composite substrate by dip-coating route. An Al_2O_3–SiO_2 sol with high solid content was selected as the raw material for mullite. The slurry of Y_2O_3 powder filled silicone resin was used to synthesize yttrium silicate. The as-fabricated coating showed high density and favorable bonding to C/SiC substrate. This group also fabricated $Y_2Si_2O_7$ coating on C/SiC composite substrate by dip-coating from Y_2O_3 powder filled silicone resin [24]. Results showed that $Y_2Si_2O_7$ coating provided excellent oxidation resistance for C/SiC substrate.

In this study, a facile sol-dipping process was developed to fabricate ZrB_2/SiO_2 coating for the oxidation protection of SiC coated C/C (SiC–C/C) composites. The heated SiC–C/C samples were dipped into the silica sol–ZrB_2 suspension system. Then, the dipped samples were treated in Ar atmosphere to form a dense ZrB_2/SiO_2 coating. Compared with the techniques as mentioned above, the sol-dipping process is a simple method to achieve uniform distribution of ZrB_2 particles in the coating. In addition, this method is energy-efficient for the preparation of ceramic coating. The sintering temperature of the ceramic coating was about 1073–1273 K. Furthermore, the sol-dipping process is suitable for the preparation of nanostructured coatings because of its low sintering temperature. The phase and morphology of the ZrB_2/SiO_2 coating prepared by the facile method were studied. The oxidation behavior and thermal shock resistance of the ZrB_2/SiO_2 coating were investigated.

2 Experimental

2.1 Fabrication of coatings

Small specimens (10 mm × 10 mm × 10 mm for the oxidation test and 55 mm × 10 mm × 4 mm for mechanical test) were cut from bulk C/C composites with a density of 1.75 g/cm^3. Then the specimens were hand-abraded using 300 grit SiC paper and cleaned with ethanol and dried at 353 K for 1.5 h. The SiC interlayer on the C/C composites was prepared by pack cementation process with Si (325 mesh), C (325 mesh), and Al_2O_3 (325mesh) powders at 1973–2273 K for 2 h in argon protective atmosphere. The details of the pack cementation process were reported in Ref. [25].

A commercial silica sol (30 wt%, pH = 9.5–10, Shanghai Second Reagent Plant, China) was used as raw material. The colloidal particle size in silica sol was about 20 nm. The ZrB_2 powder with an average

particle size of 500 nm used in this study was obtained from a commercial source (Dandong Research Institute of Chemical Industry, Liaoning, China).

The schematic for the preparation of the ZrB_2/SiO_2 coatings is shown in Fig. 1. Firstly, submicron ZrB_2 powders (25 wt%) were incorporated into the silica sol, and mechanical stirring was used constantly to get the suspension system. Secondly, the SiC–C/C samples were heated at 473 K in air for 2 min and then quickly dipped into the suspension system. The dipped samples were ultrasonically cleaned in ethanol for 3 min to remove the weakly bonded particles. Then, the above heating and impregnation process was repeated ten times. Lastly, the coated samples were treated at 1073 K for 2 h in argon atmosphere and the ZrB_2/SiO_2 coatings were prepared on the SiC–C/C samples.

In the suspension system, the colloidal silica particles with negative charge were adsorbed on the surface of the ZrB_2 particles. Solid silica gel containing well-dispersed submicron ZrB_2 powders was formed on the surface of the substrates while the heated substrates were quickly dipped into the suspension system, which transformed the ZrB_2/SiO_2 coatings after heat treatment.

2. 2 Tests and characterization

The isothermal oxidation tests of the SiC–C/C and ZrB_2/SiO_2 coated SiC–C/C samples were carried out in an electric furnace at 1773 K in air. During the isothermal oxidation test, the coated samples were taken out from the electric furnace and cooled to room temperature for several times after oxidation for a certain time. The flexural strength of the ZrB_2/SiO_2 coated SiC–C/C samples before and after oxidation was measured by a three-point bending test with a span length of 40 mm and speed of 0.5 mm/min. The thermal shock tests were carried out between 1773 K and room temperature. The coated samples were placed in a furnace and kept for 5 min, and they were immediately removed from the furnace and kept at room temperature for 5 min. After that, the samples were placed directly in the furnace for the next thermal cycle. The weight change of the samples during the oxidation and thermal shock test was measured using an electrical balance with a sensitivity of ±0.1 mg. The final mass loss percentage was obtained by computing the average values of the three samples.

The crystalline structure and morphology of the unoxidized and oxidized specimens were measured by X-ray diffraction (XRD, X'Pert PRO), scanning electron microscopy (SEM, JSM-6390A) with energy-dispersive spectroscopy (EDS).

3 Results and discussion

3. 1 Microstructure of the coating

Figure 2 shows the XRD pattern of the ZrB_2/SiO_2 coating. The prepared coatings were mainly composed of ZrB_2, SiO_2, and SiC. Minor β-SiC phase was also observed, resulting from the inner SiC layer. This suggests that the ZrB_2/SiO_2 coatings can be prepared by a facile sol-dipping approach on the SiC–C/C samples.

Figure 3(a) shows the surface morphology of the SiO_2 coating without ZrB_2 particles prepared by sol-dipping on the SiC–C/C samples. A large number of cracks can be found in the SiO_2 coating without ZrB_2 particles. The cracks split the SiO_2 coating into many discontinuous small pieces. The width of some cracks can reach about 10 μm. The magnified image (Fig. 3(b)) indicates that some small cracks have a width of about 2–3 μm. These results indicate the desiccation and calcination of silica sol shrink the SiO_2 coating and result in the

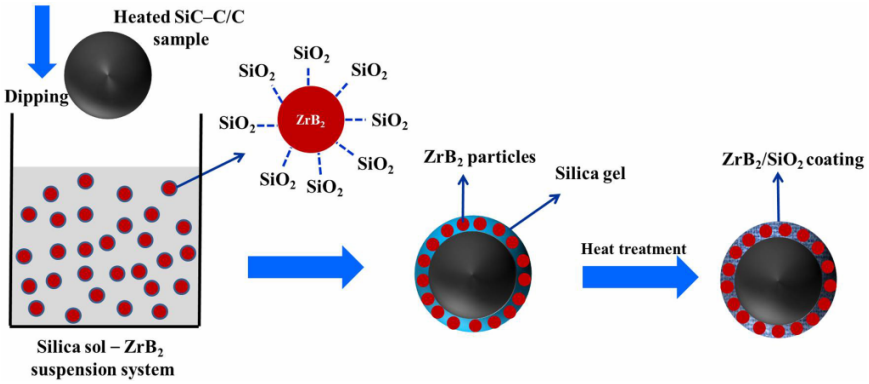

Fig. 1 Schematic for the preparation of the ZrB_2/SiO_2 coatings.

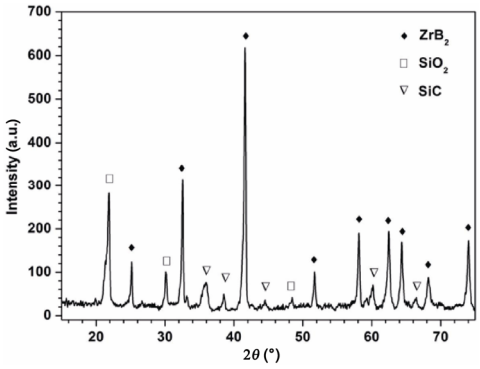

Fig. 2 XRD pattern of the ZrB_2/SiO_2 coating prepared by sol-dipping on the SiC–C/C samples.

formation of cracks. These cracks can provide the pathway for oxygen to attack C/C substrate during oxidation. In addition, these big cracks are difficult to be filled by liquid SiO_2. Therefore, the SiO_2 coating without ZrB_2 particles cannot provide good oxidation protection for the composites at high temperature.

However, the ZrB_2/SiO_2 coating presents a compact structure, and no obvious holes and cracks can be found on the coating surface, as shown in Fig. 3(c). Figure 3(d) indicates that many white particles distributed uniformly in the gray phase. According to the EDS analysis, the spot 1 was rich in element of Zr and the spot 2 was rich in element of Si (Figs. 3(e) and 3(f)). This result together with XRD analysis indicates that the white particles are the ZrB_2 phase, and the gray phase is the SiO_2 phase. The uniform distribution of the ZrB_2 particles can restrain the formation of cracks which were generated by the shrinkage of the silica gel during heat treatment.

Figure 4(a) shows the cross-section micrograph of the ZrB_2/SiO_2 coating. The coating is ~200 μm in thickness

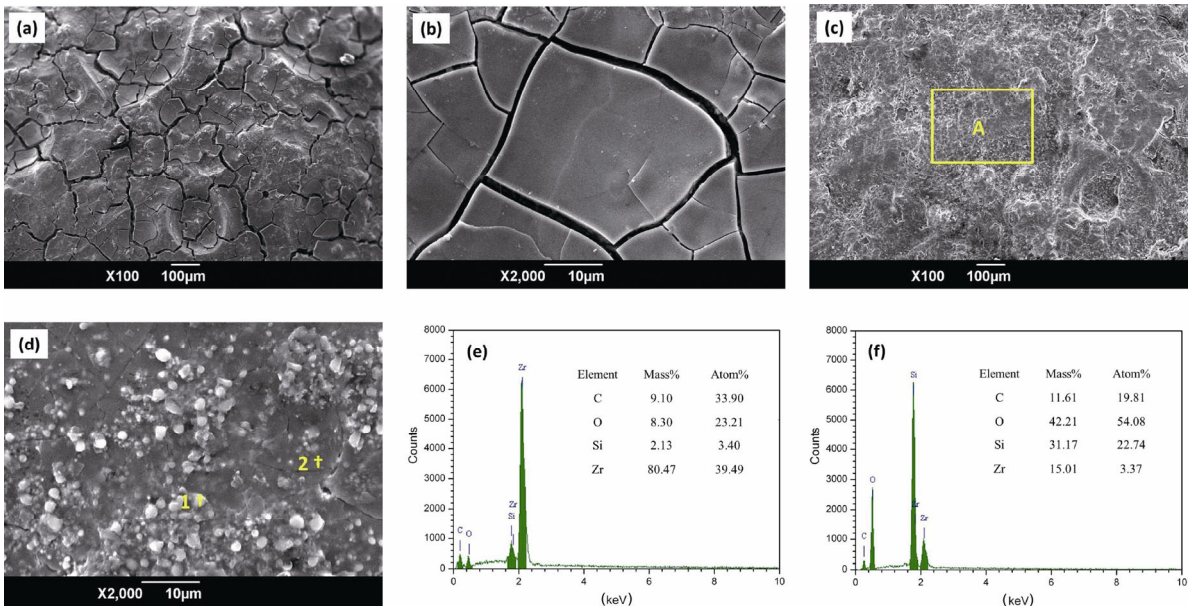

Fig. 3 (a) Surface morphology and (b) high magnification morphology of SiO_2 coating prepared by sol-dipping on the SiC–C/C samples; (c) surface morphology, (d) high magnification morphology of A, EDS of the spot 1 (e) and spot 2 (f) of the ZrB_2/SiO_2 coating prepared by sol-dipping on the SiC–C/C samples.

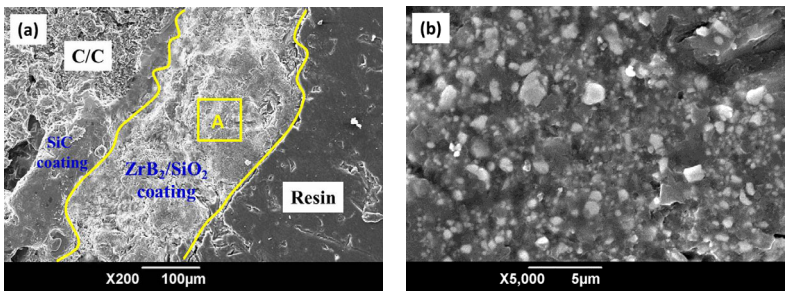

Fig. 4 (a) Cross-section morphology and (b) high magnification morphology of A of the ZrB_2/SiO_2 coating prepared by sol-dipping on the SiC–C/C samples.

without penetration cracks or big holes. The interface between the ZrB_2/SiO_2 and SiC coating was crack-free, inferring good interface bonding. Silica solid gel generated from the evaporation of silica sol can form a Si–O bond that firmly adsorbs on the surface, which improves the cohesion of the ZrB_2/SiO_2 coating and the interfacial bonding with SiC coating. The particle size ranges from sub-micrometers to several micrometers (Fig. 4(b)). The tiny ZrB_2 particles present a uniform distribution in the coatings. Therefore, the compact ZrB_2/SiO_2 coatings with uniformly dispersed ZrB_2 particles were prepared by the sol-dipping approach on the SiC–C/C samples, which was expected to have good oxidation protective property at high temperature.

3. 2 Oxidation resistance of the coated samples

Figure 5 shows the isothermal oxidation curves of the coated samples at 1773 K in air. The ZrB_2/SiO_2 coating can provide excellent oxidation protection for SiC–C/C composites. The weight loss of the ZrB_2/SiO_2 coated SiC–C/C specimens was 6.9 mg/cm^2 after oxidation at 1773 K in air for 160 h, while the weight loss of SiC–C/C specimens is up to 9.7 mg/cm^2 after oxidation for only 60 h. The oxidation behavior of the ZrB_2/SiO_2 coated specimens at 1773 K could be divided into four processes marked as A, B, C, and D. The transition time for the four processes was 6, 20, and 160 h. The coated specimens exhibited a weight increase at the initial oxidation stage (process A), and the weight increase of the coated specimens exhibited a decreasing trend after 6 h (process B). Then the coated specimens presented a slow weight loss (process C). Finally, the coated specimens showed a sharp weight loss with 22.4 mg/cm^2 after oxidation at 1773K for 180 h, indicating the failure of the ZrB_2/SiO_2 coating (process D).

Figure 6 shows the XRD pattern of the ZrB_2/SiO_2 composite coatings after oxidation at 1773 K for 160 h. The $ZrSiO_4$, ZrO_2, and SiO_2 phases can be found in the XRD pattern. The formation of ZrO_2 indicates that the ZrB_2 particles in the coating were oxidized. The $ZrSiO_4$ was formed by the reaction between SiO_2 and ZrO_2 after oxidation. The formation of $ZrSiO_4$ is beneficial to the oxidation resistance ability because of its low permeability of oxygen and high thermal stability under high temperature. Moreover, the $ZrSiO_4$ and ZrO_2 phases existing in the coating can reduce the consumption of SiO_2 and then improve the oxidation resistance of C/C composites at high temperature [2,26].

The surface SEM image of the ZrB_2/SiO_2 coating after oxidation at 1773 K for 160 h is shown in Fig. 7(a). A continuous glass layer is formed and exhibits coarse morphology. No holes and cracks can be observed in the glass layer. Many submicron white particles dispersed uniformly in the continuous gray glass layer (Fig. 7(b)). The XRD analysis demonstrates that the white particles are ZrO_2 and $ZrSiO_4$, and the gray glass phase is SiO_2. Therefore, a continuous SiO_2 glass layer embedded with ZrO_2 and $ZrSiO_4$ particles was formed after the oxidation at 1773 K for 160 h. The continuous SiO_2 glass layer embedded with ZrO_2 and $ZrSiO_4$ particles presents good stability and small diffusion rate of oxygen, thus improving the oxidation resistance of the coated samples [27,28]. The cross-section SEM image showed that the coating is dense and little glass phase can be found after oxidation at 1773 K for 160 h (Fig. 7(c)). The thickness of the coating is ~180–200 μm, which is similar to that of the coating before oxidation. The uniformly dispersed ZrO_2 and $ZrSiO_4$ particles also exist in the cross-section of the coating (Fig. 7(d)). Besides, cracks or pores cannot be found in the coating.

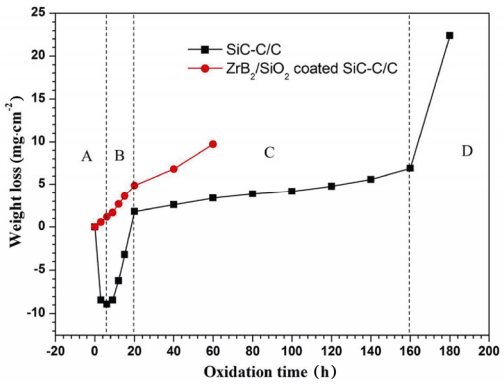

Fig. 5 Isothermal oxidation curves of the SiC–C/C and ZrB_2/SiO_2 coated SiC–C/C composites at 1773 K in air.

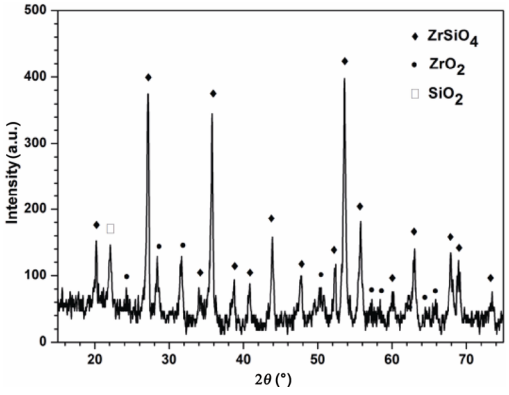

Fig. 6 XRD pattern of the ZrB_2/SiO_2 coating after oxidation at 1773 K for 160 h.

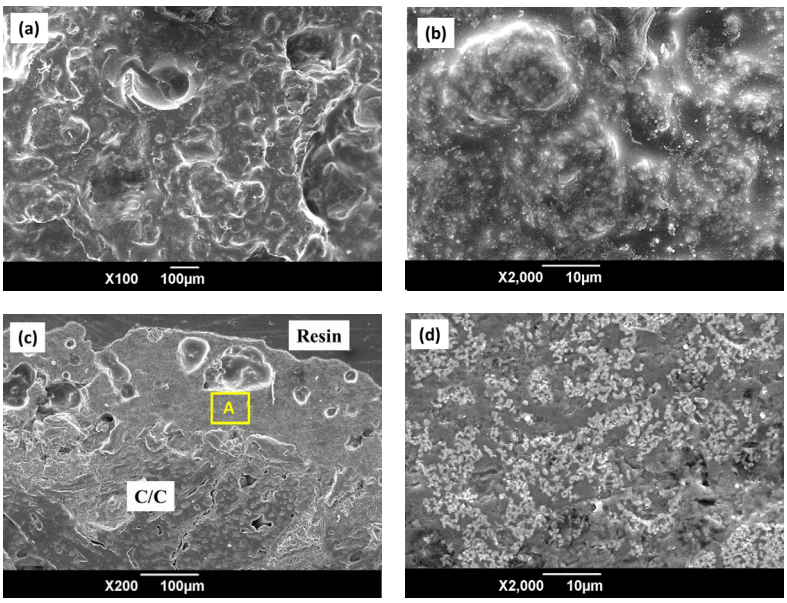

Fig. 7 (a) Surface morphology, (b) high magnification morphology of surface, (c) cross-section morphology, and (d) high magnification morphology of area A of the ZrB_2/SiO_2 coating after oxidation at 1773 K for 160 h.

However, the appearance of glass phase inside the coating indicated that the oxidizing atmosphere has diffused into ZrB_2/SiO_2 coating at 1773 K for 160 h.

Cracks and many holes are formed on the surface of the coating when the coated sample is oxidized at 1773 K for 180 h (Fig. 8(a)). A large number of holes also generated in the inner part of the coating (Fig. 8(b)). The partial SiC inner coating is also oxidized. The formation of holes results from the volatilization of SiO_2 glass phase as well as the release of the gaseous byproducts. These results indicated that the oxygen diffuses into the coating and causes the oxidation of the inner part of the ZrB_2/SiO_2 coating. Therefore, the ZrB_2/SiO_2 coating prepared by facile sol-dipping can protect the composites from being oxidized for 160 h at 1773 K.

Figure 9 presents load–displacement curves of the ZrB_2/SiO_2 coated SiC–C/C composites before and after oxidation for 160 h at 1773 K. The curve after oxidation illustrates a typical pseudo-plastic fracture behavior, just as it was before oxidation. The flexural strength of the ZrB_2/SiO_2 coated composites before and after oxidation is 98.6±6.5 and 85.7±5.8 MPa, respectively. The flexural strength retention ratio of the ZrB_2/SiO_2 coated composites is 87% after oxidation for 160 h at 1773 K. After the oxidation at 1773 K for 160 h, no visible holes and cracks can be observed in the SiO_2 glass layer. The cross-section morphology of the coating is dense and little glass phase can be found.

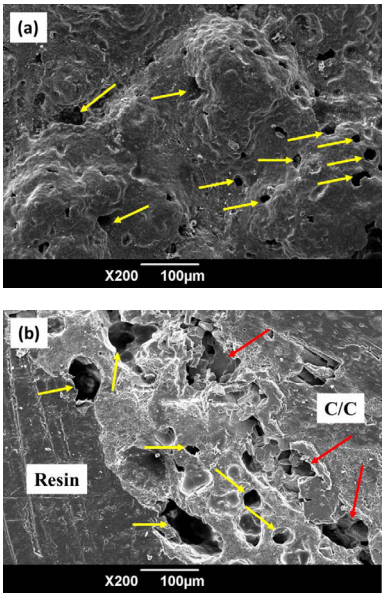

Fig. 8 (a) Surface and (b) cross-section morphology of the ZrB_2/SiO_2 coating after oxidation at 1773 K for 180 h.

Moreover, the thickness of the coating is similar to that of the coating before oxidation. However, there is a slow weight loss trend during oxidation for 160 h at 1773 K and the formation of glassy phase, which decreases the flexural strength of the composites slightly after oxidation.

3. 3 Oxidation resistance mechanism of the coating

The following reactions occur during the oxidation in the ZrB_2/SiO_2 coated SiC–C/C composites [29,30].

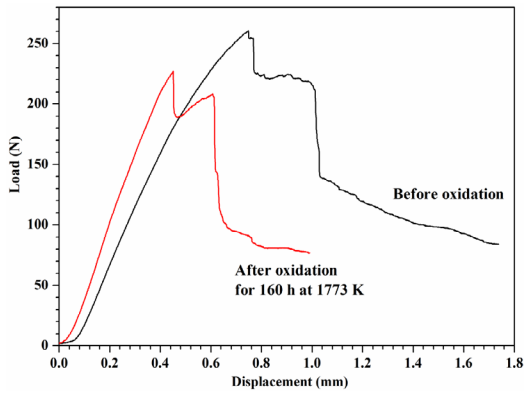

Fig. 9 Load–displacement curves of the ZrB_2/SiO_2 coated SiC–C/C composites before and after oxidation for 160 h at 1773 K.

$$2ZrB_2(s)+5O_2(g) \rightarrow 2ZrO_2(s)+2B_2O_3(l) \quad (1)$$

$$SiO_2(s) \rightarrow SiO_2(l) \rightarrow SiO_2(g) \quad (2)$$

$$SiC(s)+2O_2(g) \rightarrow SiO_2(l)+CO_2(g) \quad (3)$$

$$ZrO_2(s)+SiO_2(s) \rightarrow ZrSiO_4(s) \quad (4)$$

$$2C(s)+O_2(g) \rightarrow 2CO(g) \quad (5)$$

$$C(s)+O_2(g) \rightarrow CO_2(g) \quad (6)$$

According to the above reactions, the oxidation of ZrB_2 and SiC leads to a net mass gain. The weight loss of the sample results from the oxidation of C/C composites and evaporation of B_2O_3 and SiO_2 in the oxidation process [18]. Figure 10 shows the schematic of the oxidation resistance mechanism of the ZrB_2/SiO_2 coating. The weight gain of the coating is observed in the process A, which is mainly due to the oxidation of ZrB_2 forming the ZrO_2 and liquid B_2O_3. Meanwhile, the SiO_2 particles in the ZrB_2/SiO_2 coating initiate to form liquid SiO_2. The formation of liquid B_2O_3 and SiO_2 leads to the healing of the microcracks in the coating and improves the oxidation resistance. In the process B, the liquid B_2O_3 would volatilize rapidly with the increase of oxidation time. So, the weight gain of the coated specimens exhibited a decreasing trend. After being oxidized for 20 h, the weight loss was only 1.8 mg/cm^2, which showed the outstanding oxidation resistance of the coating.

With increasing oxidation time (process C), SiO_2 glassy layer, ZrO_2, and $ZrSiO_4$ particles were formed. The ZrO_2 and $ZrSiO_4$ particles were embedded in the SiO_2 glassy layer. The continuous SiO_2 glassy layer generates on the surface of the coating, which can efficiently fill the defects in the coating and protect the specimens from oxidation. The coated specimens present a slow weight loss trend, indicating a remarkable oxidation resistance of the coating. Moreover, the ZrO_2 and $ZrSiO_4$ particles embedded in the SiO_2 glassy layer act as pinning particles restraining generation of microcracks [31]. Furthermore, the $ZrSiO_4$ particles embedded in the SiO_2 glassy layer can lower the diffusion rate of oxygen and improve the stability of the SiO_2 glassy layer, which improves the oxidation resistance of the coated samples at 1773 K [32].

When the coating was oxidized for 180 h (process D), liquid SiO_2 will rapidly volatilize. Some oxygen can penetrate the glass layer or pass the microcracks and cause the oxidation of the inner part of the coating, thus forming a large number of holes in the coating, as indicated by the yellow arrows in Fig. 8. These holes were difficult to be filled because of the volatilization of liquid SiO_2. Therefore, the oxidizing atmosphere can diffuse to SiC coated C/C sample rapidly along with the holes, which also form a large number of holes in the SiC inner coating, as indicated by red arrows in Fig. 8(b). Thus, the oxidation curve of the coating shows an abrupt growth trend, indicating that the coating has failed to protect the C/C substrate.

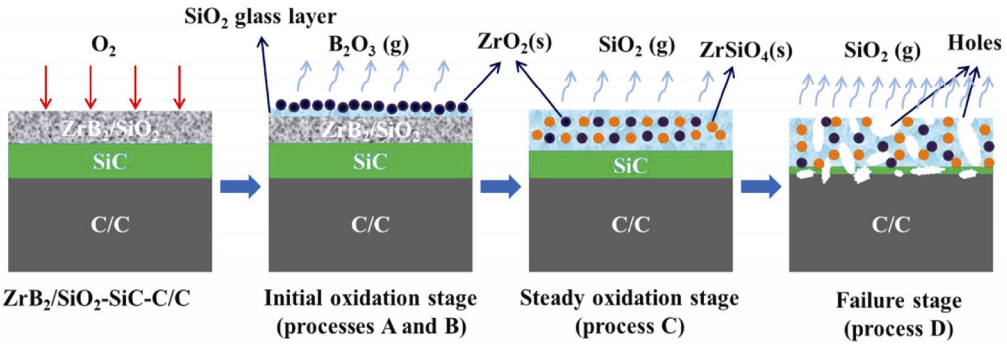

Fig. 10 Schematic of the oxidation resistance mechanism of the ZrB_2/SiO_2 coating.

3. 4 Thermal shock resistance of the coated samples

The thermal shock resistance of ZrB_2/SiO_2 coatings is investigated between 1773 K and room temperature, as shown in Fig. 11. The weight loss of the ZrB_2/SiO_2 coated sample presents linear relationship. The slope of the line is 0.422, and the final weight loss per unit area is 6.35 mg/cm^2.

Figure 12(a) shows the surface morphology of the ZrB_2/SiO_2 coated sample after 15 times thermal shocks. Cracks and pores can be observed on the coating surface, which can provide the pathway for oxygen to attack C/C substrate during thermal cycling. During the thermal shock tests, the thermal stress would cause the cracking of the coating which could be attributed to the thermal expansion coefficient mismatch between coating and substrate [33]. The cross-sectional morphology of the ZrB_2/SiO_2 coated sample after 15 times thermal shocks is shown in Fig. 12(b). Penetrative cracks distributed in the failed coating after thermal shock test. Under the failed coating, the SiC inner coating and C/C substrate were oxidized. Besides, the cracks can be found between the ZrB_2/SiO_2 coating and SiC inner coating, indicating the ZrB_2/SiO_2 coating de-bonded from the substrate. The penetrative cracks and the de-bonded coating interface provide channels for oxygen diffusion. With thermal shock test carrying on, the cracks propagate along the interface. Finally, the coating would fail to protect for the C/C substrate.

In summary, the sol-dipping process can achieve a uniform distribution of fine ZrB_2 particles in the ZrB_2/SiO_2 coatings. This method has the following advantages for the preparation of ceramic coating. Firstly, sol-dipping is a convenient method for preparation of coating consisting of ceramic nanoparticles. There are fewer restrictions to the shape of the substrate samples. The samples are heated and immersed in the suspension consisting of ceramic nanoparticles and silica sol. The coating can be formed on the area that contacted with the silica sol. Secondly, this method is energy efficient for the preparation of the ceramic coating. The sintering temperature of the ceramic coating was 1073–1273 K. Furthermore, the sol-dipping process is suitable for preparation of nanostructured coatings because of its low sintering temperature. Therefore, the sol-dipping process provides a new idea for the preparation of nanostructured ceramic coatings with low cost, which has the industrial application prospect in the field of high-temperature oxidation resistance and wear resistant coating.

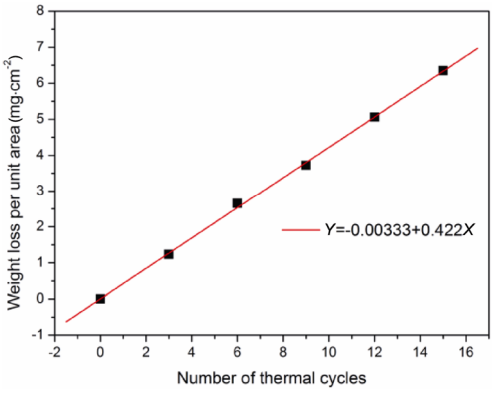

Fig. 11 Weight loss curves of the coated C/C samples during thermal cycling between 1773 K and room temperature.

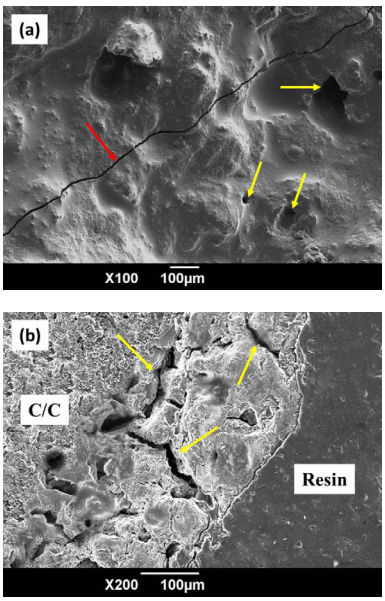

Fig. 12 (a) Surface and (b) cross-section micrographs of the ZrB_2/SiO_2 coating after 15 thermal cycles between 1773 K and room temperature.

4 Conclusions

A ZrB_2 particles reinforced glass (ZrB_2/SiO_2) coating was prepared on the SiC–C/C composites by a facile sol-dipping approach. The coating with ~200 μm in thickness presented a compact structure, and no obvious holes and cracks could be found. The uniform distribution of ZrB_2 particles can restrain the extension of the cracks generated shrinkage of the silica gel during the heat treatment. The ZrB_2/SiO_2 coating protected the composites from oxidation for 160 h at 1773 K with a weight loss of 6.9 mg/cm^2. The flexural strength of the ZrB_2/SiO_2 coated composites before and after oxidation

is 98.6±6.5 and 85.7±5.8 MPa, respectively. The flexural strength retention ratio of the ZrB_2/SiO_2 coated composites is 87% after oxidation for 160 h at 1773 K. The continuous SiO_2 glass layer embedded with the $ZrSiO_4$ and ZrO_2 submicron particles was formed during oxidation, which could lower the diffusion rate of oxygen and improve the stability of the SiO_2 glass layer. Therefore, the ZrB_2/SiO_2 coating presented good oxidation protective (resistance) property. After thermal cycles between 1773 K and room temperature for 15 times, the weight loss of the ZrB_2/SiO_2 coated sample presented linear relationship. The penetrative cracks and the de-bonded coating interface could be found in the failed coating after the thermal shock test. This resulted in the failure of the ZrB_2/SiO_2 coating to protect the C/C substrate.

Acknowledgements

This research was supported by the National Natural Science Foundation of China (Grant Nos. 51302160 and 51402177), the Science and Technique Talent Project of Shaanxi Province (Grant No. 2016KJXX-07), Natural Science Foundation of Shaanxi Province (Grant No. 2018JM5038), Natural Science Foundation of Education Department of Shaanxi Province (Grant No. 14JK1103), and Research Foundation of Shaanxi University of Science & Technology (Grant No. BJ14-20).

References

[1] Xu B, He R, Hong C, *et al.* Ablation behavior and mechanism of double-layer ZrB_2-based ceramic coating for lightweight carbon-bonded carbon fiber composites under oxyacetylene flame at elevate temperature. *J Alloys Compd* 2017, **702**: 551–560.

[2] Purwar A, Basu B. Thermo-structural design of ZrB_2–SiC-based thermal protection system for hypersonic space vehicles. *J Am Ceram Soc* 2017, **100**: 1618–1633.

[3] Zhou S, Qi Y, Wang P, *et al.* A ZrB_2–SiC/SiC oxidation protective dual-layer coating for carbon/carbon composites. *Adv Appl Ceram* 2017, **116**: 462–467.

[4] Yang X, Li W, Wang S, *et al.* ZrB_2 coating for the oxidation protection of carbon fiber reinforced silicon carbide matrix composites. *Vacuum* 2013, **96**: 63–68.

[5] Niu Y, Wang Z, Zhao J, *et al.* Comparison of ZrB_2–$MoSi_2$ composite coatings fabricated by atmospheric and vacuum plasma spray processes. *J Therm Spray Tech* 2017, **26**: 100–107.

[6] Fu Q-G, Jing J-Y, Tan B-Y, *et al.* Nanowire-toughened transition layer to improve the oxidation resistance of SiC–$MoSi_2$–ZrB_2 coating for C/C composites. *Corros Sci* 2016, **111**: 259–266.

[7] Silvestroni L, Sciti D. Densification of ZrB_2–$TaSi_2$ and HfB_2–$TaSi_2$ ultra-high-temperature ceramic composites. *J Am Ceram Soc* 2011, **94**: 1920–1930.

[8] Yao X-Y, Li H-J, Zhang Y-L, *et al.* A SiC/ZrB_2–SiC/SiC oxidation resistance multilayer coating for carbon/carbon composites. *Corros Sci* 2012, **57**: 148–153.

[9] Li K, Hu M, Dynamic oxidation resistance and residual mechanical strength of ZrB_2–$CrSi_2$–SiC–Si/SiC coated C/C composites. *Ceram Int* 2017, **43**: 4880–4887.

[10] Feng T, Li H-J, Shi X-H, *et al.* Oxidation and ablation resistance of ZrB_2–SiC–Si/B-modified SiC coating for carbon/carbon composites. *Corros Sci* 2013, **67**: 292–297.

[11] Hwang SS, Vasiliev AL, Padture NP. Improved processing and oxidation-resistance of ZrB_2 ultra-high temperature ceramics containing SiC nanodispersoids. *Mat Sci Eng A* 2007, **464**: 216–224.

[12] Yao X, Li H, Zhang Y, *et al.* A SiC–Si–ZrB_2 multiphase oxidation protective ceramic coating for SiC-coated carbon/carbon composites. *Ceram Int* 2012, **38**: 2095–2100.

[13] Pourasad J, Ehsani N, Valefi Z. Oxidation resistance of a SiC–ZrB_2 coating prepared by a novel pack cementation on SiC-coated graphite. *J Mater Sci* 2017, **52**: 1639–1646.

[14] Li L, Li H, Yin X, *et al.* Microstructure evolution of SiC–ZrB_2–ZrC coating on C/C composites at 1773 K under different oxygen partial pressures. *J Alloys Compd* 2016, **687**: 470–479.

[15] Wang L, Fu Q-G, Zhao F-L. A novel gradient SiC–ZrB_2–$MoSi_2$ coating for SiC coated C/C composites by supersonic plasma spraying. *Surf Coat Technol* 2017, **313**: 63–72.

[16] Niu Y, Wang H, Li H, *et al.* Dense ZrB_2–$MoSi_2$ composite coating fabricated by low pressure plasma spray (LPPS). *Ceram Int* 2013, **39**: 9773–9777.

[17] Yang X, Li W, Wang S, *et al.* ZrB_2/SiC as a protective coating for C/SiC composites: Effect of high temperature oxidation on mechanical properties and anti-ablation property. *Composites Part B* 2013, **45**: 1391–1396.

[18] Ouyang H, Li C, Huang J, *et al.* Self-healing ZrB_2–SiO_2 oxidation resistance coating for SiC coated carbon/carbon composites. *Corros Sci* 2016, **110**: 265–272.

[19] Yao X, Tan S, Huang Z, *et al.* Dispersion of talc particles in a silica sol. *Mater Lett* 2005, **59**: 100–104.

[20] Tomas M, Amaveda H, Angurel LA, *et al.* Effect of silica sol on the dispersion–gelation process of concentrated silica suspensions for fibre-reinforced ceramic composites. *J Eur Ceram Soc* 2013, **33**: 727–736.

[21] Zhu X, Jiang D, Tan S, *et al.* Dispersion properties of alumina powders in silica sol. *J Eur Ceram Soc* 2001, **21**: 2879–2885.

[22] Santana I, Pepe A, Jimenez-Pique E, *et al.* Corrosion protection of carbon steel by silica-based hybrid coatings containing cerium salts: Effect of silica nanoparticle content. *Surf Coat Technol* 2015, **265**: 106–116.

[23] Ma Q, Cai L. Fabrication and oxidation resistance of

mullite/yttrium silicate multilayer coatings on C/SiC composites. *J Adv Ceram* 2017, **6**: 360–367.

[24] Ma Q, Cai L. Fabrication of $Y_2Si_2O_7$ coating and its oxidation protection for C/SiC composites. *Trans Nonferrous Met Soc China* 2017, **27**: 390–396.

[25] Fu Q-G, Li H-J, Shi X-H, *et al.* Silicon carbide coating to protect carbon/carbon composites against oxidation. *Scripta Mater* 2005, **52**: 923–927.

[26] Wang L, Fu Q, Zhao F, A novel gradient SiC–ZrB_2–$MoSi_2$ coating for SiC coated C/C composites by supersonic plasma spraying. *Surf Coat Technol* 2017, **313**: 63–72.

[27] Yang X, Li W, Wang S, *et al.* Ablative property of ZrC–SiC multilayer coating for PIP-C/SiC composites under oxy-acetylene torch. *Ceram Int* 2012, **38**: 2893–2897.

[28] Pourasad J, Ehsani N. In-situ synthesis of SiC–ZrB_2 coating by a novel pack cementation technique to protect graphite against oxidation. *J Alloys Compd* 2017, **690**: 692–698.

[29] Jin H, Meng S, Zhang X, *et al.* Oxidation of ZrB_2–SiC–graphite composites under low oxygen partial pressures of 500 and 1500 Pa at 1800 ℃. *J Am Ceram Soc* 2016, **99**: 2474–2480.

[30] Ouyang G, Ray PK, Kramer MJ, *et al.* High-temperature oxidation of ZrB_2–SiC–AlN composites at 1600 ℃. *J Am Ceram Soc* 2016, **99**: 808–813.

[31] Ren X, Li H, Chu Y, *et al*. Preparation of oxidation protective ZrB_2–SiC coating by in-situ reaction method on SiC-coated carbon/carbon composites. *Surf Coat Technol* 2014, **247**: 61–67.

[32] Zhang Y, Hu H, Zhang P, *et al.* SiC/ZrB_2–SiC–ZrC multilayer coating for carbon/carbon composites against ablation. *Surf Coat Technol* 2016, **300**: 1–9.

[33] Fan X, Huang W, Liu H, *et al.* Bond stability and oxidation resistance of BSAS-based coating on C/SiC composites. *Surf Coat Technol* 2017, **309**: 35–46.